Biomedicine & Pharmacotherapy 116 (2019) 109017

Contents lists available at ScienceDirect

Biomedicine & Pharmacotherapy

journal homepage: www.elsevier.com/locate/biopha

# *Heamatococcus pluvialis* ameliorates bone loss in experimentally-induced osteoporosis in rats via the regulation of OPG/RANKL pathway

Farouk K. El-Baz[a], Dalia O. Saleh[b,*], Gehad A. Abdel Jaleel[b], Rehab A. Hussein[c], Azza Hassan[d]

[a] Plant Biochemistry Department, National Research Centre (NRC), 33 El Buhouth St. (Former El Tahrir St.), Dokki, Giza P.O.12622, Egypt
[b] Pharmacology Department, National Research Centre (NRC), 33 El Buhouth St. (Former El Tahrir St.), Dokki, Giza P.O.12622, Egypt
[c] Pharmacognosy Department, National Research Centre (NRC), 33 El Buhouth St. (Former El Tahrir St.), Dokki, Giza P.O.12622, Egypt
[d] Pathology Department, Faculty of Veterinary Medicine, Cairo University, Giza, Egypt

ARTICLE INFO

*Keywords:*
*Heamatococcus pluvialis*
Osteoporosis
Bone mineral density
osteoprotegerin
RANKL
Rats

ABSTRACT

*Backgrounds:* Osteoporosis prevailing in elderly involves a marked increase in bone resorption showing an initial fall in bone mineral density leading to a significant reduction in bone formation.
*Aim:* The present study aimed to investigate the effect of *Heamatococcus pluvialis* microalgae on osteoporosis in D-galactose-treated rats. The underlying mechanism was tracked targeting the osteoprotegerin (OPG)/ nuclear factor-κβ ligand (RANKL) pathway using micro-computed tomography scanning.
*Methods:* Osteoporosis was induced in rats by intraperitoneal injection of D-galactose (200 mg/kg/day) for eight consecutive weeks. Osteoporotic rats were orally treated with *H. pluvialis* biomass (BHP; 450 mg/kg), its polar (PHP; 30 mg/kg) and carotenoid (CHP; 30 mg/kg) fractions for the last 2 weeks of D-Gal injection. Twenty four hours after the last dose of the treatments, tibia bones of the rats were scanned using micro-computed tomography scanning for bone mineral density (BMD), bone volume fraction (BV/TV), trabecular thickness/separation/number (Tb.Th, Tb.Sp, Tb.N) evaluation, blood samples were withdrawn and sera were used for biochemical assessment. Moreover, femur bones were examined histopathologically using several stains.
*Results:* Induction of osteoporosis was associated with a marked reduction in BMD, BV/TV, Tb.Th, Tb.Sp, Tb.N and in serum levels of phosphorus and catalase. On the other hand, a significant elevation in serum levels of calcium, bone alkaline phosphatase (BALP) and interleukin-6 was observed. Moreover, up-regulation of OPG was detected in osteoporotic rats. Oral treatment with BHP, and PHP incremented tibia BMD and serum phosphorus level along with the decrease in serum levels of calcium, BALP, interleukin-6, OPG and RANKL. However, treatment with CHP almost restored all the fore mentioned parameters to normal values. Furthermore, the histopathological evaluation emphasized the biochemical outcomes.
*Conclusion: H. pluvialis* fractions rich in astaxanthin ameliorated bone loss in experimentally-induced osteoporosis in rats probably through the down-regulation of serum OPG in concurrence with up-regulation of serum RANKL.

## 1. Introduction

Osteoporosis is characterized by low bone mass and micro architectural deterioration of bone tissue which results in bone fragility and consequently increases fracture risk [1]. On advanced age, the rate of bone turnover increases in both genders at the tissue level leading to an impairment in osteoblastic bone formation along with an increase in osteoclastic bone resorption [2,3].

Free radical and oxidative stress theory of aging is recognized as one of the most plausible and convincing explanations for the process of aging and are involved in inflammatory arthritis and age-related bone loss D-galactose is known to cause oxidative stress and induce aging-related diseases by induction of lipid peroxidation and mitochondrial dysfunction. This results in further increase in the production of reactive oxygen species (ROS) and osteoclasts differentiation through upregulation of the receptor activator of nuclear factor-κβ ligand (RANKL) which is a signaling pathway that is essential for osteoclast differentiation, activation and survival [4].

Osteoprotegerin (OPG); a decoy receptor for RANKL produced by osteoblasts, shows high affinity and competes with RANK for RANKL binding and thus functions as an inhibitor of RANK-RANKL interaction and inhibits osteoclast maturation and activation. Thus, OPG prevents

* Corresponding author.
*E-mail address:* doabdelfattah@yahoo.com (D.O. Saleh).

https://doi.org/10.1016/j.biopha.2019.109017
Received 25 July 2018; Received in revised form 20 May 2019; Accepted 21 May 2019

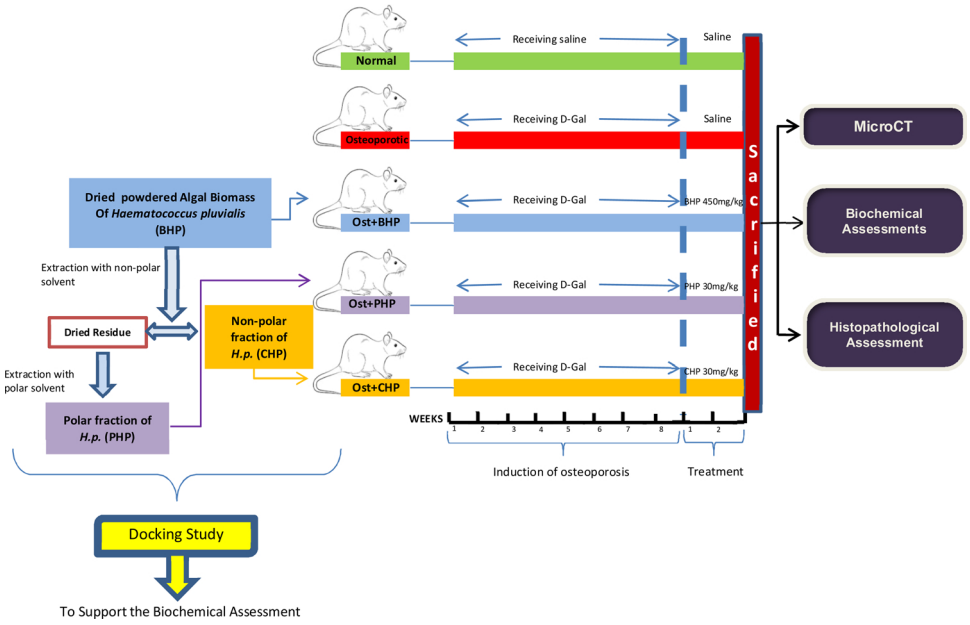


**Fig. 1.** Flowchart of *H. pluvialis* biomass, its polar, and its non-polar fractions extraction routine, docking study and the pharmacological study experimental design.

RANKL from binding to and activating RANK and also inhibits the development of osteoclasts and down-regulates the RANKL signaling through RANK [5].

*Heamatococcus pluvialis*; a microalgae belonging to Chlorophyta, family Haematococcaceae is well known for its high content of the potent antioxidant astaxanthin. Astaxanthin possesses a variety of pharmacological activities; protective effect against asthma, inflammation and liver damage [6]. The high antioxidant effect of *H. pluvialis* drew attention to the possible interference with the high oxidative stress associated with aging and consequently with osteoporosis as one of its manifestations.

The aim of the present study was to investigate the ameliorative effect of *H. pluvialis* biomass, carotenoid and polar fractions on osteoporosis in D-galactose treated rats and to assess the underlying mechanism targeting the OPG/ RANKL pathway using micro-computed tomography scanning.

## 2. Material and methods

### 2.1. Preparation of algal material

The dried biomass of *H. pluvialis* was obtained from Algal Technology Lab., NRC. It was grinded thoroughly for cell wall disruption. The dried powder was subjected to successive extraction using petroleum ether (40–60 °C) till exhaustion to render a non-polar fraction. The residue is allowed to dry and further extracted with 70% methanol till exhaustion to render a polar fraction. Both fractions were dried under reduced pressure in a rotatory evaporator under a temperature not exceeding 40 °C. The dried fractions were kept in dark bottles at a temperature less than 4 °C. The phytoconstituents of the non-polar fraction were investigated using LC-DAD/ESI-MS in our previous work [7]. The non-polar fraction was found to be rich in carotenoids the most abundant of which was astaxanthin (49.99 mg total astaxanthin per 100 g) in free and in esterified form [8] as illustrated in Fig. 1.

### 2.2. Docking study

Docking calculations were carried out using MOE. The MMFF94 force field was used for energy minimization of ligand molecule (all-trans astaxanthin) using MOE. Gasteiger partial charges were added to the ligand atom. Non-polar hydrogen atoms were merged, and rotatable bonds were defined. Docking calculations were carried out on OPG-RANKL complex protein model. Essential hydrogen atoms, Kollman united atom type charges, and solvation parameters were added. Affinity (grid) maps of 20 × 20 × 20 Å grid points and 0.375 Å spacing were generated using the Autogrid program. AutoDock parameter set- and distance-dependent dielectric functions were used in the calculation of the van der Waals and the electrostatic terms, respectively. Docking simulations were performed using the Lamarckian genetic algorithm (LGA) and the Solis & Wets local search method.

### 2.3. Biological assay

#### 2.3.1. Animals

Male albino rats weighing 130–150 g were obtained from the animal house colony of the National Research Centre. They was kept and housed under suitable environmental conditions throughout the period of investigation; ambient temperature (25 ± 2 °C), humidity (60 ± 10%), and alternating 12 h light-dark cycles. Rats was fed a standard rat pellet diet and allowed free access to water.

#### 2.3.2. Experimental design

Osteoporosis was induced in rats by intraperitoneal injection with D-Gal (200 mg/kg/day) for eight consecutive weeks according to the method described by [9]. Thirty albino rats were assigned into five groups, each group includes six rats. Group I served as a negative control group receiving no treatment, group II served as positive control which received D-Gal, while groups III, IV and V received D-Gal then orally treated with *H. pluvialis* biomass (BHP; 450 mg/kg; p.o.), its polar fraction (PHP; 30 mg/kg; p.o.) and carotenoid fraction (CHP; 30 mg/kg; p.o.), respectively for the last 2 weeks of D-Gal injection (fractions doses were calculated according to their yield) as illustrated in Fig. 1.

Twenty-four hours after the last dose of the *H. pluvialis* treatments, blood samples were withdrawn from the retro-orbital plexus at the same time intervals. Moreover, femur and tibia bones were removed; tibia bone scanned by with a micro-CT scanner and femur preserved in 10% formalin/saline and used for histopathological examination.

#### 2.3.3. Micro-computed tomography scanning

Samples were scanned with a micro-CT scanner (GE eXplore Locus SP Micro-CT; GE Healthcare, Waukesha, WI, USA) with a 16-μm voxel

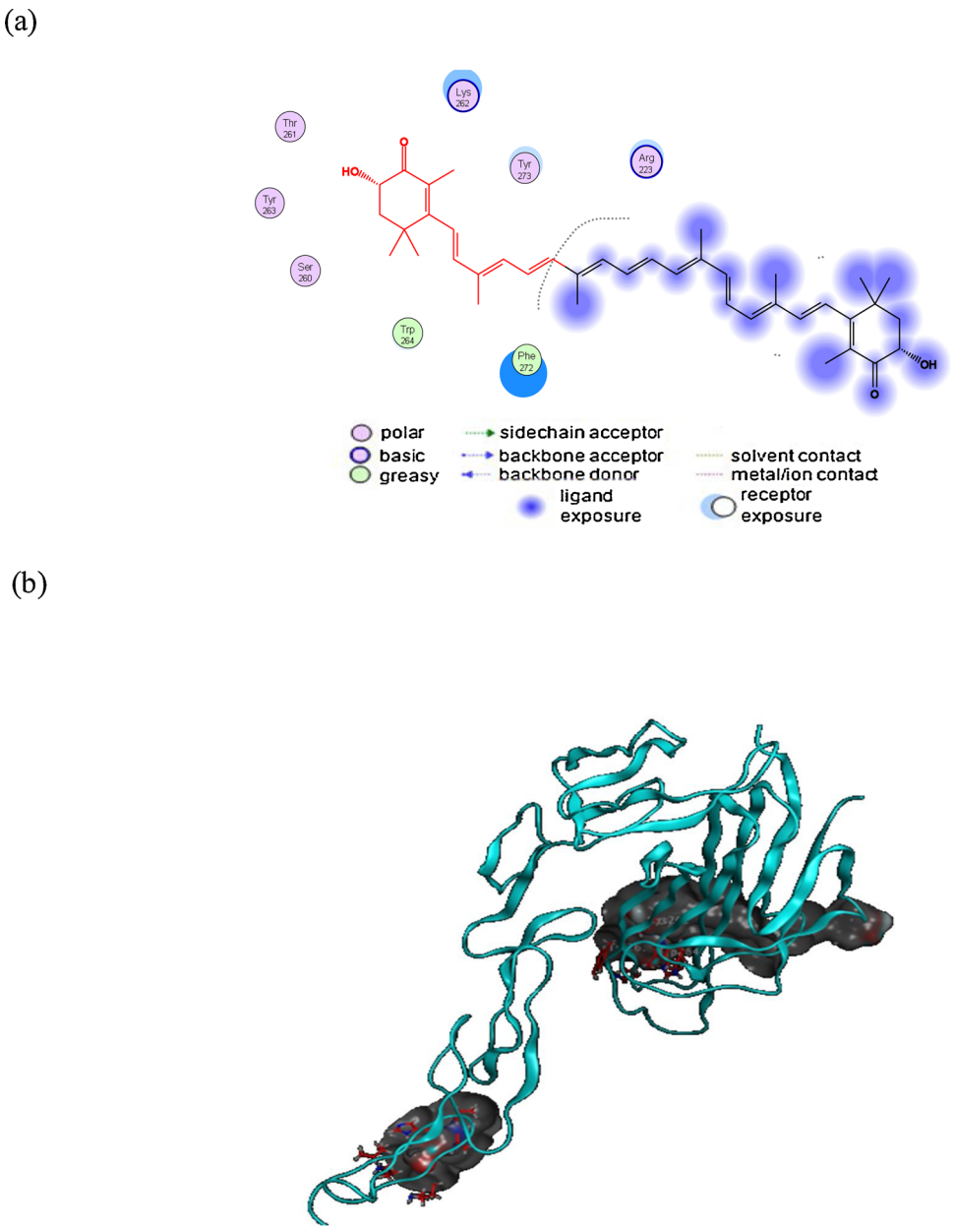


**Fig. 2.** Plot of the interaction (a) and docking of astaxanthin on active sites of OPG-RANKL complex protein (b).

size. The scanning procedure lasted about 1 h per sample and generated approximately 700 images of 1024 × 1024 pixels. Three-dimensional microarchitecture of the alveolar bone was analyzed using MicroView ABA 2.2 (GE Healthcare). The grayscale CT images were segmented using a constrained Gaussian filter (sigma = 1.2, support = 2) to remove noise, and a fixed threshold (25.5% of maximal grayscale value) was used to extract the mineralized tissue structure. Morphological measurements, including bone mass density (BMD), bone volume fraction (BV/TV), trabecular thickness/separation/number (Tb.Th, Tb.Sp and Tb.N) were estimated.

### 2.3.4. Biochemical parameters

Serum levels of calcium and phosphorus were measured colorimetrically at 585 nm according to the method described by Goonasekera et al. [10] and at 640 nm according to the method described by Dai et al. [11], respectively. Additionally, bone specific alkaline phosphatase (BALP), osteoprotegrin (OPG) and nuclear factor-κβ ligand (RANKL) were determined by enzyme immunoassay according to Tahtela et al. [12], Pineda et al. [13] and Hofbauer et al. [14], respectively. Catalase and interleukin 6 were also measured by enzyme immunoassay and the concentrations were expressed as pg/ml according to [15] and [16], respectively.

### 2.3.5. Histopathological examination

Femur bones were dissected and fixed in 10% formaldehyde/saline after the removal of soft tissue. The bones were decalcified in formic acid for 3 weeks, and were kept for histopathological examination using H & E stain. The thickness of bone trabeculae was estimated in 15 random high power field/group. Furthermore, alizarin red and alkaline phosphatase stains; an osteoblast differentiation marker, were used for morphometric analysis. The number of osteoblasts; the mean osteoblasts count (N.Ob), in a square area 155,327.7μm$^2$ in 10 fields was counted. The mean grey levels in 10 fields were also measured using the interactive measurement software of the system on a total magnification of (100X). The results appear automatically on the monitor in the form of count, distant measured in (um) and grey level ranging from 0 white to 255 black.

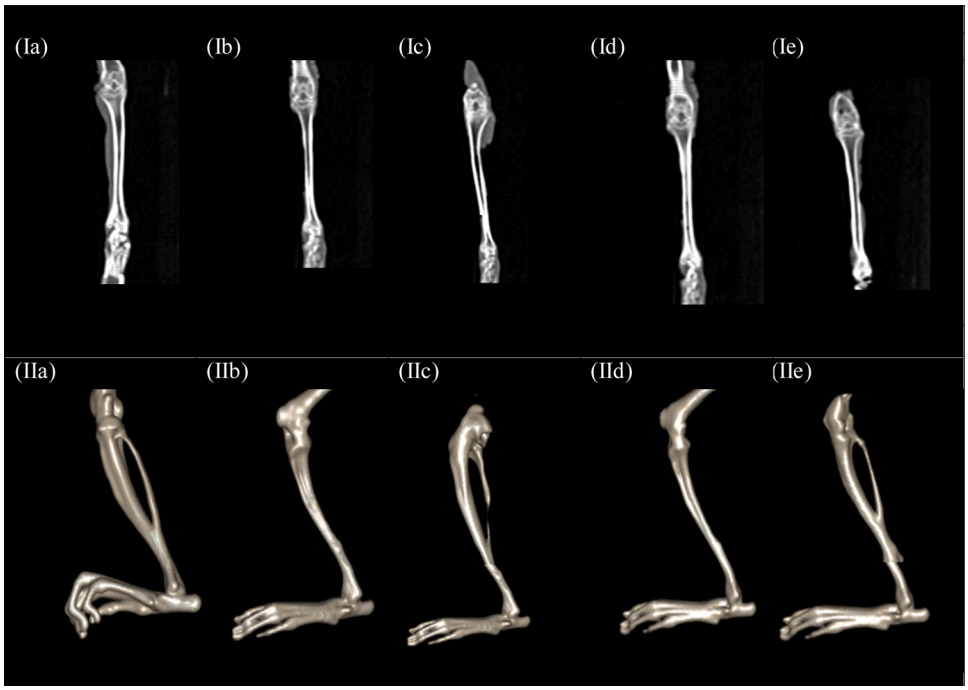


**Fig. 3.** Effect of *H. pluvialis* on the micro-architecture of tibia bone in D-galactose induced osteoporotic rats analyzed by μCT. (a) Bone isolated from normal rat; (b) Bone isolated from osteoporotic rat; (c, d & e) Bone isolated from osteoporotic rat treated with BHP, PHP and CHP, respectively. Images (Ia-e) representing two-dimensional plane; Images (IIa-e) representing three-dimensional plane.

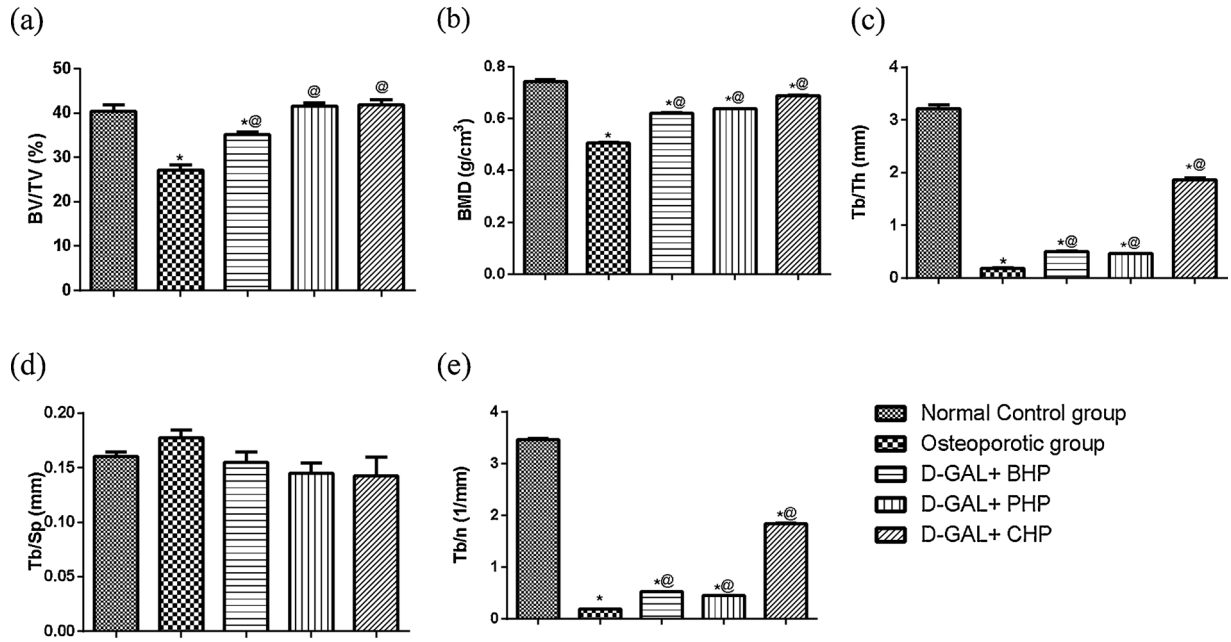


**Fig. 4.** Effect of *H. pluvialis* on the microarchitecture of tibia bone in D-galactose induced osteoporotic rats analyzed by μCT. The figure illustrates: bone volume fraction (BV/TV) (a), bone mineral density (BMD) (b), trabecular thickness (Tb/Th) (c), trabecular separation (Tb/Sp) (d) and trabecular number (Tb/N) (e). Data are represented as mean ± SEM. Statistical analysis was carried out by one-way analysis of variance (ANOVA) followed by Tukey-Kramer test for multiple comparisons. (n = 6–8) *Significantly different from normal control group at $P \leq 0.5$. $^{@}$ Significantly different from osteoporotic group at $P \leq 0.5$.

#### 2.3.6. Statistical analysis

Data was expressed as means ± SEM. Statistical significance was taken as $p < 0.05$, using one-way analysis of variance (ANOVA) followed by Tukey-Kramer multiple comparisons test to verify the difference between various groups.

## 3. Results

### 3.1. Docking study

The docking of all-trans astaxanthin; the major carotenoid found in *H. pluvialis*; on OPG-RANKL complex protein showed that it possesses high affinity towards OPG-RANKL complex where the estimated free energy of binding −6.2676 kcal/mol as illustrated in Fig. 2.

### 3.2. Pharmacological study

#### 3.2.1. Effects of H. pluvialis on microarchitectural parametric values of tibia of osteoporotic rat detected by micro-CT imaging

Two and three dimensional planes have been imaged using. μ-CT imaging thst morphologically shows trabecular bone and cortical bone as shown in Fig. 3. Briefly; intraprotonial injection of normal rats with

**Table 1**
Effect of *H. pluvialis* on serum levels of calcium, phosphorus and bone alkaline phosphatase (BALP) in D-galactose induced osteoporotic rats.

| Groups | Serum calcium (mg/dl) | Serum Phosphorus (mg/dl) | BALP (pg/ml) |
|---|---|---|---|
| Normal control group | 10.95 ± 0.25 | 4.62 ± 0.096 | 5.67 ± 0.34 |
| Osteoporotic group | 20.76 ± 1.03* | 2.28 ± 0.064* | 14.40 ± 0.89* |
| Osteoporotic group + BHP (450 mg/kg) | 16.38 ± 0.27*,@ | 3.57 ± 0.02*,@ | 12.67 ± 0.48* |
| Osteoporotic group + PHP (30 mg/kg) | 15.84 ± 0.13*,@ | 4.07 ± 0.05*,@ | 9.01 ± 0.59*,@ |
| Osteoporotic group + CHP (30 mg/kg) | 12.18 ± 1.08@ | 4.53 ± 0.06@ | 8.65 ± 0.88*,@ |

Osteoporosis was induced in rats by intraproteonial injection of D-galactose (200mg/kg) for 8 consecutive weeks. Osteoporotic rats were orally treated with *H. pluvialis* biomass, its polar and its non-polar fractions for 14 days. Twenty four hours after the last dose of the extracts, blood samples were withdrawn from the retro-orbital plexus, centrifugated and the sera were used for estimation of calcium, phosphorus and BALP levels.
Data are represented as mean ± SEM. Statistical analysis was carried out by one-way analysis of variance (ANOVA) followed by Tukey-Kramer test for multiple comparisons. (n = 6–8).
* Significantly different from normal control group at P ≤ 0.5.
@ Significantly different from osteoporotic group at P ≤ 0.5.

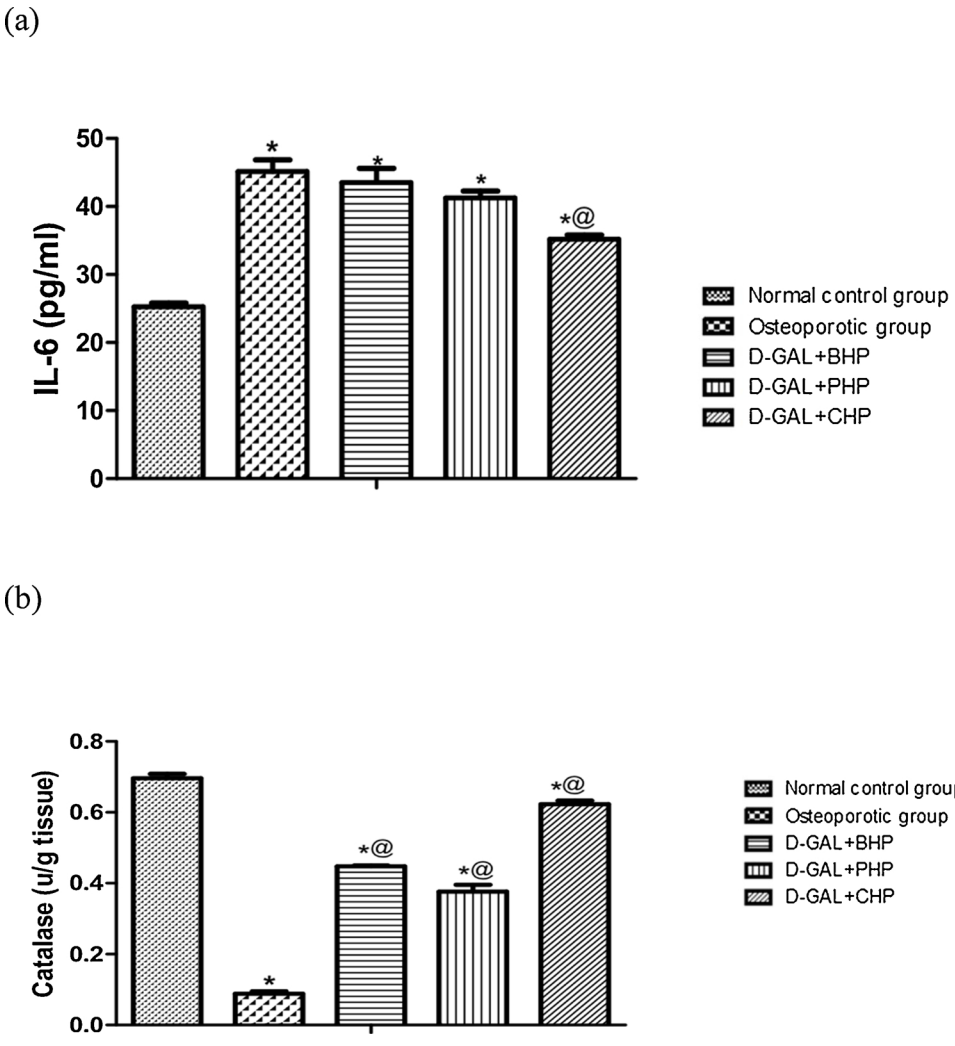


**Fig. 5.** Effect of *H. pluvialis* on serum interleukin-6 (a) and catalase (b) in D-galactose induced osteoporotic rats. Osteoporosis was induced in rats by intraproteonial injection of D-galactose (200mg/kg) for 8 consecutive weeks. Osteoporotic rats were orally treated with *H. pluvialis* biomass (BHP; 450 mg/kg), its polar (PHP; 30 mg/kg), and its non-polar fractions (CHP; 30 mg/kg), for 14 days. Twenty four hours after the last dose of the extracts, blood samples were withdrawn from the retro-orbital plexus, centrifugated and the serum were used for interleukin-6 estimation. Data are represented as mean ± SEM. Statistical analysis was carried out by one-way analysis of variance (ANOVA) followed by Tukey-Kramer test for multiple comparisons. (n = 6–8). *Significantly different from normal control group at P ≤ 0.5. @ Significantly different from osteoporotic group at P ≤ 0.5.

D-galactose for eight consecutive weeks led dramatic to decline in the tibia BMD by about 32% as compared to normal control group. Oral treatment of osteoporotic rats with BHP (450 mg/kg), PHP (30 mg/kg) and CHP (30 mg/kg) for 14 days incremented the tibia BMD by about 23%, 26% and 36%, respectively, as compared to the osteoporotic control group as presented by Fig. 4.

Statistical analysis of the microarchitectural parameters indicated prominent decrease in BV/TV, Tb.Th., and Tb.N. of the tibia bone between normal and D-galactose injected rats by 32%, 94% and 95%, respectively; with no change estimated in the Tb.Sp. Treatment of osteoporotic rats with BHP (450 mg/kg) elevated the BV/TV, Tb.Th., and Tb.N. of the tibia bone by 33%, 1.6 and 1.7 folds respectively. Similarly, PHP (30 mg/kg) and CHP (30 mg/kg; p.o) showed an elevation in the Tb.Th., and Tb.N. by 1.4 and 8 folds, respectively. However, oral treatment of PHP (30 mg/kg) and CHP (30 mg/kg) for 14 days augmented the tibia BV/TV reaching nearly the normal values as presented by Fig. 4.

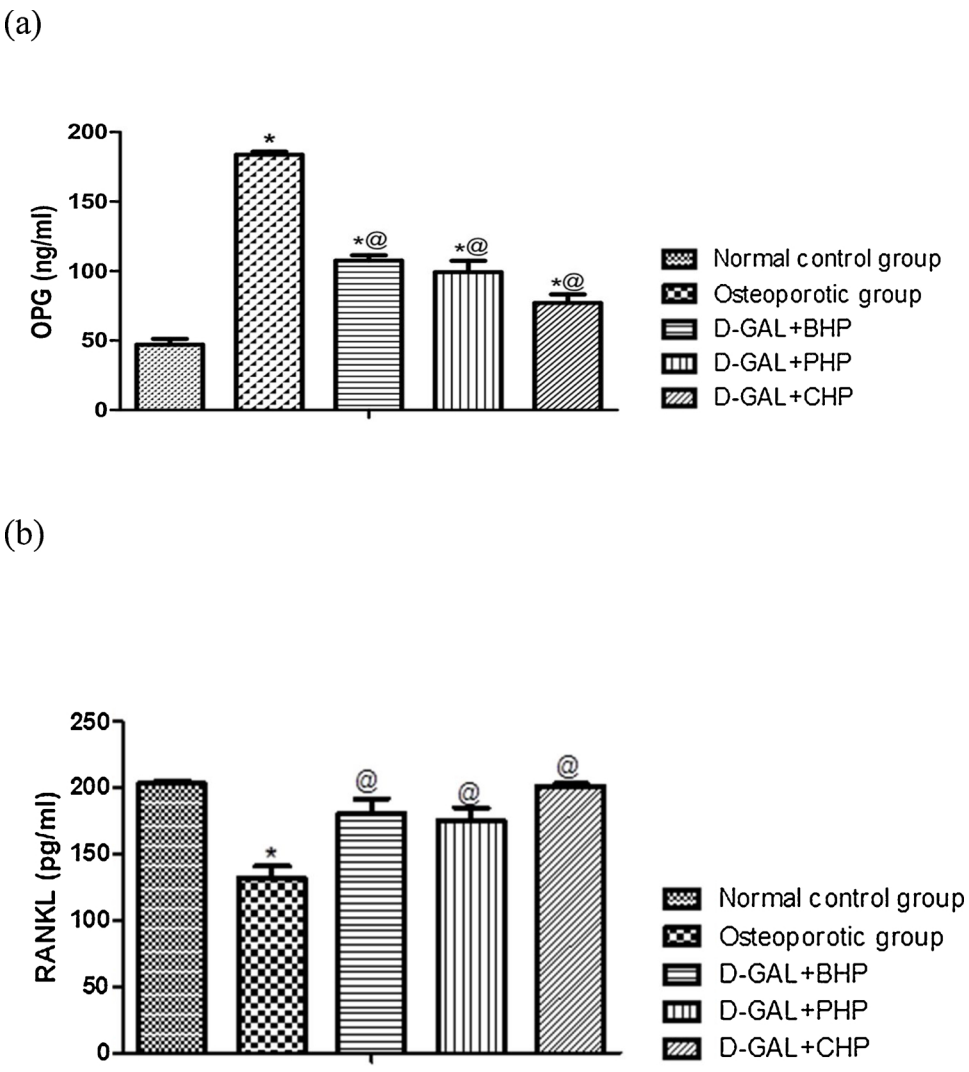


**Fig. 6.** Effect of *H. pluvialis* on serum osteoprotegerin (OPG) (a) and RANKL (b) in D-galactose induced osteoporotic rats. Osteoporosis was induced in rats by intraproteonial injection of D-galactose (200mg/kg) for 8 consecutive weeks. Osteoporotic rats were orally treated with *H. pluvialis* biomass (BHP; 450 mg/kg), its polar (PHP; 30 mg/kg), and its non-polar fractions (CHP; 30 mg/kg), for 14 days. Twenty four hours after the last dose of the extracts, blood samples were withdrawn from the retro-orbital plexus,centrifugated and the serum were used for osteoprotegerin estimation. Data are represented as mean ± SEM. Statistical analysis was carried out by one-way analysis of variance (ANOVA) followed by Tukey-Kramer test for multiple comparisons. (n = 6–8). *Significantly different from normal control group at $P \leq 0.5$. [@] Significantly different from osteoporotic group at $P \leq 0.5$.

*3.2.2. Effects of H. pluvialis on serum levels of calcium, phosphorus bone alkaline phosphatase (BALP) of osteoporotic rats*

D-galactose treated rats exhibited a marked elevation of serum calcium level by nearly 2 folds as compared to the normal control group. Treatment with BHP (450 mg/kg) and PHP (30 mg/kg) for 14 days elevated serum calcium levels by 21% and 23% after 2 weeks, respectively, as compared to the osteoporotic control. Similarly, administration of CHP (30 mg/kg; p.o) showed a dramatic elevation in serum calcium level by about 41% showing no significant difference from the normal rats as shown in Table 1.

Moreover, the present results revealed that induction of osteoporosis was associated with a decline in serum phosphorus level by 50%, as compared to the normal control group. Administration of BHP (450 mg/kg) and PHP (30 mg/kg) for 14 days showed marked increase in serum phosphorus level by 57% and 79%, respectively as compared to the osteoporotic rats. Similarly, osteoporotic rats treated with CHP (30 mg/kg; p.o) normalized the serum phosphorus level after 2 weeks of treatment as represented in Table 1.

Serum BALP was augmented by nearly 2.5 folds after 8 weeks of D-galactose injection as compared to normal control group. A prominent decline in serum BALP was observed after administration of both BHP and CHP by 37% and 40%, respectively, as compared to the osteoporotic group which is presented in Table 1.

*3.2.3. Effects of H. pluvialis on serum levels of interleukin-6 and catalase of osteoporotic rats*

Osteoporosis was associated with a marked increase in serum interleukin-6 level by 78% with respect to the normal group. Oral treatment of osteoporotic rats with CHP (30 mg/kg) for 2 weeks showed a pronounced decline in serum interleukin-6 by 22% as illustrated in Fig. 5a.

Induction of osteoporosis for was accompanied with a dramatic decrease in serum catalase level by about 87% as compared to the normal control group. Serum catalase level was significantly elevated after oral treatment with BHP (450 mg/kg), PHP (30 mg/kg) and CHP (30 mg/kg) for 2 weeks by 4, 3 and 6 folds respectively after 2 weeks as compared to the osteoporotic control group. However, the carotenoid fraction of *H. pluvialis* nearly restored the serum level of catalase to the normal value as graphically illustrated in Fig. 5b.

*3.2.4. Effects of H. pluvialis on serum levels of osteoprotegerin (OPG) and nuclear factor-κβ ligand (RANKL) of osteoporotic rats*

Osteoporotic rats showed a pronounced elevation in serum levels of OPG and RANKL by 3.8 folds and 35%, respectively, with respect to the normal control group. Oral administration of BHP (450 mg/kg), PHP (30 mg/kg) or CHP (30 mg/kg) depicted a reduction of OPG levels by 41%, 46% and 58%, respectively as compared to the osteoporotic control group as illustrated in Fig. 6a. Similarly, treatment of these rats with BHP (450 mg/kg), PHP (30 mg/kg) or CHP (30 mg/kg) succeeded

**Table 2**
Effect of *H. pluvialis* on mean thickness of bone trabeculae in D-galactose induced osteoporotic rats.

| Parameters<br>Groups | Mean thickness of bone trabeculae ($\mu$m/HPF) | Mean osteoblast count (N.Ob/155327.7$\mu m^2$) | Mean grey level |
|---|---|---|---|
| **Normal control group** | 133.22±8.28 | 31 | 157.6 |
| **Osteoporotic group** | 55.25±5.52* | 23 | 184.7 |
| **Osteoporotic group + BHP (450 mg/kg)** | 83.78±7.9*@ | 26 | 185.06 |
| **Osteoporotic group + PHP (30 mg/kg)** | 130.52a ±8.2@ | 30 | 158.9 |
| **Osteoporotic group + CHP (30 mg/kg)** | 92.66b±6.98*@ | 28 | 174.33 |

Osteoporosis was induced in rats by intraproteonial injection of D-galactose (200mg/kg) for 8 consecutive weeks. Osteoporotic rats were orally treated with *H. pluvialis* biomass, its polar and its non-polar fractions for 14 days. Twenty four hours after the last dose of the extracts, the animals were sacrified, the bones were dissected and fixed in 10% formaldehyde/saline after the removal of soft tissue. The bones were decalcified in formic acid for 3 weeks, and were kept for histopathological examination using H & E stain and alkaline phosphatase stain. The thickness of bone trabeculae were estimated in 15 random high power field (HPF)/group and the mean osteoblasts count (N.Ob/155,327.7μm$^2$) and grey level were estimated per square area 155,327.7μm$^2$. Mean thickness of bone trabeculae are represented as mean ± SEM. Statistical analysis was carried out by one-way analysis of variance (ANOVA) followed by Tukey-Kramer test for multiple comparisons.
*Significantly different from normal control group at P ≤ 0.5.
@ Significantly different from osteoporotic group at P ≤ 0.5.

to normalize the serum RANKL levels as illustrated in Fig. 6b.

*3.2.5. Effects of H. pluvialis on histopathological examination of osteoporotic rats*

The histopathological specimens were examined for the integrity of the periosteum and endosteum, the proliferation of the fibrous layer in response to treatment as well as the defects of inner endosteum, indicating attempts of regeneration and improvement. Lacunae of the osteoblasts widening indicates under laying pathology, the more the widening and its persistence the more deteriorated the case is. The mean thickness of bone trabculae recorded in the normal and treated group is illustrated in Table 2.

Normal rats showed normal bone epiphyseal structure with normal bone trabeculae (Fig. 7a) with normal quiescent osteoblast (Fig. 7b). The mean thickness of bone trabeculae recorded in this group is 133.22 ± 8.28 μm (Fig. 7a & b). The N.Ob/155,327.7μm$^2$ and the grey level are recorded in alkaline phosphatase-stained sections 31 and 157.60, respectively (Table 2 and Fig. 9a–c). On the other side, bone of D-galactose-treated rats revealed apparent thinning of bone trabrculae, with mean bone thickness of 55.25 ± 5.52 μm, and with remarkable increase of the marrow fat (adipogenesis) in addition to marked bone resorption represented by presence of numerous osteoclasts on the surface of the trabeculae (Fig. 7c & d) as well as increased micro cracks in the bone. One of the characteristic histopthological alterations demonstrated in this group was reduction of the bone mineralization rate indicated by the number of mineralized nodules in osteoporotic group was less than that in normal that are confirmed in alizarin red-stained sections (Fig. 7c & d) compared to the normal group (Fig. 7a & b). The mean N.Ob/155,327.7μm$^2$ and the grey level are recorded in alkaline phosphatase-stained sections 23 and 184.7, respectively (Table 2 and Fig. 9d–f).

Examination of bone sections obtained from osteoporotic rats treated with BHP (450 mg/kg), PHP (30 mg/kg) or CHP (30 mg/kg) revealed reparative and regenerative changes, however, bone sections obtained from osteoporotic rats treated with BHP (450 mg/kg) revealed showed marked regression of osteoclastic activity together with increased thickness of the trabeculae reaching a mean of 83.78 ± 7.9 μm (Fig. 7e & f). Alizarin red stained sections revealed mild increase in the bone mineralization rate (Fig. 8e & f). The N.Ob/155,327.7μm$^2$ and the grey level are recorded in alkaline phosphatase-stained sections 26 and 185.06, respectively (Table 2 and Fig. 9g–i). Likewise, variable areas of bone sections obtained from rats treated with PHP (30 mg/kg) revealed prominent increase of bone trabeculae with remarkable activation and proliferation of osteoblasts which appeared plump with abundant basophilic cytoplasm (Fig. 7g &h). The mean thickness of bone trabeculae is 130.52 ± 8.2 μm (Fig. 7g & h). The bone trabeculae are more intensely stained with Alizarin red compared to the D-galactose treated group (Fig. 8g & h). The N.Ob/155,327.7μm$^2$ and the grey level are recorded 30 and 158.9, respectively (Table 2 and Fig. 9j–l).

Similarly, bone sections obtained from osteoporotic rats treated with CHP (30 mg/kg) revealed thickening of bone trabeculae with a mean of 92.66 ± 6.98 μm as well as increased osteoblastic activity and diminished osteoclasts (Fig. 7i & j). Increased bone density was demonstrated in this group, in which the bone trabeculae appeared intensely red indicating high bone mineralization rate (Fig. 8i & j). The N.Ob/155,327.7μm$^2$ and the grey level are recorded in alkaline phosphatase-stained sections 28 and 174.33, respectively (Table 2 and Fig. 9m, n &o).

## 4. Discussion

Aging is accompanied by bone deterioration regarding composition, architecture and function, thus predisposes osteoporosis [17]. Aging process of bone and osteoporosis are closely related thus recently,

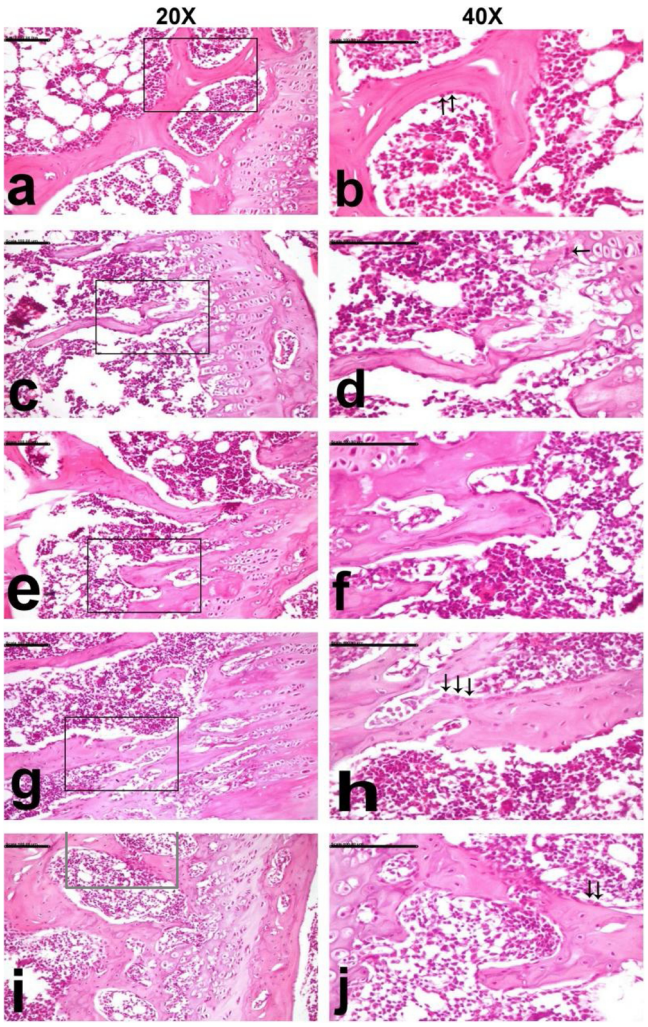


**Fig. 7.** Effect of *H. pluvialis* on bone histopathological examination of D-galactose induced osteoporotic rats using H&E stain. Bone tissue of, (a & b) normal rats showing normal epiphyseal structure with normal bone trabeculae (a) with normal quiescent osteoblast (arrows) (b), (c & d) D-galactose treated rats showing apparent thinning of bone trabeculae (c) with presence of multinucleated osteoclasts on the surface of the trabeculae (d), (e,f) *H. pluvialis* biomass (BHP; 450 mg/kg) group showing increased thickness of the trabeculae, (g & h), Polar fractions (PHP; 30 mg/kg) group showing prominent increase of bone trabeculae (g) with remarkable activation and proliferation of osteoblasts which appeared plump with abundant basophilic cytoplasm (arrows) (h), and (i & j)), and non-polar fractions (CHP; 30 mg/kg) group showing thickening of bone trabeculae with increased osteoblastic activity (arrows) and diminished osteoclasts. (stain: H&E, scale bar 100um).

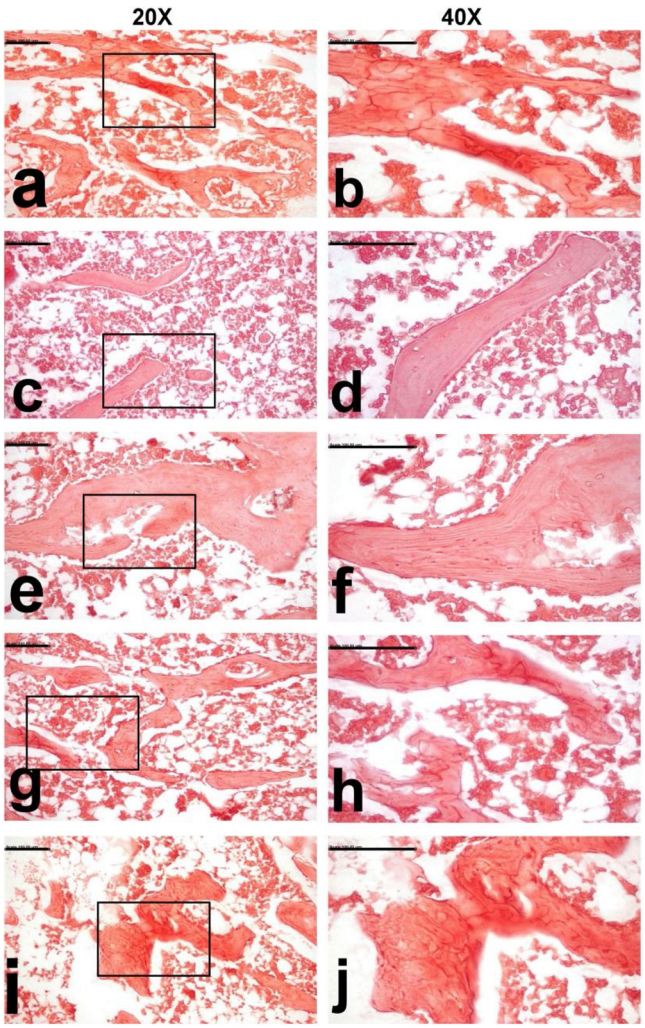


**Fig. 8.** Effect of *H. pluvialis* on bone histopathological examination of D-galactose induced osteoporotic rats using Alizarin red stain. Photomicrograph of bone tissue of (a & b) normal rats showing strong mineralization, (c & d) D-galactose treated rats showing very weak mineralization line, (e & f) *H. pluvialis* biomass (BHP; 450 mg/kg) group showing mild mineralization, (g & h) polar fractions (PHP; 30 mg/kg) group showing increased mineralization, and (i & j), and non-polar fractions (CHP; 30 mg/kg) group showing strong mineralization. (stain: Alizarin red, scale bar 100um).

research on the mechanisms of age-related bone loss has been elevated dramatically [18].

Despite osteoporosis is mostly viewed from the scope of sex hormonal decline especially in women, age-related osteoporosis or bone aging attracts much attention in attempts for defining the underlining mechanisms. In the current study, aging induced by D-galactose (200 mg/kg) for 8 weeks rendered the rats osteoporotic which is a well-established model of age-related bone loss and is considered an appropriate way to study bone changes in humans [19]. This model has shown increased serum levels of calcium and BALP together with decreased serum phosphorus.

The current work revealed that the three-dimensional reconstructed micro-CT images showed an intuitive view of prominent alteration of the bone of D-galactose injected rats showing dramatic bone loss manifested by reduction in the tibia BMD, BV/TV, Tb.Th and Tb.N. These alterations are considered as a result of elevation in alveolar bone turnover among the osteoporotic in comparison to the normal rats. These results are in accordance with those of previous studies [20,21]. Reduction of the bone mineralization rate has been confirmed by Alizarin red-stained sections compared to the normal group.

Thus, indicating a state of osteoporosis that has emphasized by a significant alteration in serum calcium/ phosphorus levels; as expressed in the elevation of the former and the decline of the latter, accompanying D-galactose induced osteoporosis. The change in serum calcium and phosphorus homeostasis which is common in elderly could be attributed to vitamin D deficiency that directly causes bone loss through activation of osteoclastic cells leading to the influx of the extracellular fluid carrying calcium ions thus decreasing the secretion of parathyroid hormone (PTH) [22]. The decline in serum PTH and

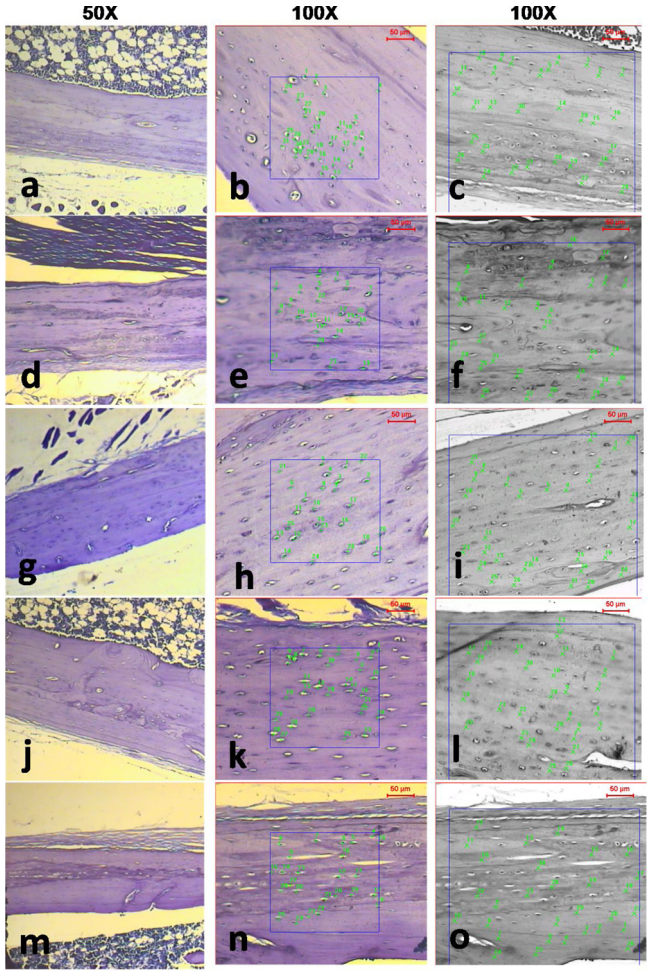


**Fig. 9.** Effect of *H. pluvialis* on bone histopathological examination of D-galactose induced osteoporotic rats using alkaline phosphatase stain. Photomicrograph of bone tissue of (a, b & c) normal rats, (d, e & f) D-galactose treated rats showing decrease in the mean oesteoblastic count with elevated grey level, (g, h & i) *H. pluvialis* biomass (BHP; 450 mg/kg) group, (j, k & l) polar fractions (PHP; 30 mg/kg) group and (m, n & o), and non-polar fractions (CHP; 30 mg/kg) group showed an increase in the mean oesteoblastic count with a reduction in the grey level. (stain: Alkaline phosphatase, scale bar 50um).

vitamin D further leads to decrease in the intestinal calcium and phosphorus absorption [23–25].

As a result of reduction in calcium absorption during osteoporosis, the mineralization of calcium by BALP was inhibited hence elevating the levels of these bone formation markers in blood circulation [26]. Moreover, osteoblasts normally express large amounts of the bone isoenzyme of alkaline phosphatase, and serum levels are usually elevated when osteoblastic activity and bone formation rates are increased [27]. Such increments can also be attributed to the osteoclastic break down of bone matrix [28].

In the current study, treatment with BHP and PHP elevated serum calcium level and decreased serum phosphorus level as compared to the osteoporotic rats. Similarly, administration of CHP showed a pronounced elevation in serum calcium level and normalized the serum phosphorus level. Low bone mass which is a major risk factor for fractures [29] was dramatically reduced in the present study in D-galactose injected rats demonstrated the induction of osteoporosis. The 3-D bone microstructure analysis using micro-CT demonstrated significant changes in BMD, BV/TV, Tb.Th and Tb.N indicating alleviation in the alveolar bone loss in groups treated with BHP, PHP and CHP for 14 consecutive days with respect to D-galactose injected rats. These results were confirmed by the histopathological examination of bone sections obtained from osteoporotic rats treated with BHP (450 mg/kg), PHP (30 mg/kg) or CHP (30 mg/kg) which revealed regenerative alterations. Furthermore, the result of alizarin red staining showed that the number of mineralized nodules in osteoporotic group was less than that in treated ones thus indicating an increase in the bone mineralization rate [30]. Similarly, alkaline phosphatase staining which is an osteoblast differentiation marker [31,32] confirmed the fore mentioned results; whereas the count of osteoblastic cells has been boosted by oral treatment of osteoporotic rats with *H. pluvialis* for 2 consecutive weeks the presenting stimulation of osteoblastic cell proliferation. This mechanism has been illustrated in Fig. 10.

Osteoporosis was also accompanied with augmentation in interleukin-6 level. Accelerated osteoclastic activity and bone resorption in osteoporotic rats in the current work was prominently clarified by the increased level of osteoclastogenic cytokine interleukin-6 which was previously reported in experimental animals [33] and in postmenopausal women [34].

Oral treatment of osteoporotic rats with carotenoid fraction of *H. pluvialis* for 2 weeks showed a pronounced decline in serum interleukin-6. [35] assured that the development of agents that modulate the actions of interleukin-6 may provide alternative osteoporosis management strategy than existing general osteoporosis therapies [35]. Moreover a recent study indicated that blockade of interleukin-6 signaling may prevent tumor-induced bone remodeling thus decreasing fractures [36]. It has been reported that astaxanthin and astaxanthin-rich products are commonly indicated as immune modulators probably by suppressing IκB Kinase-dependent NF-κB activation [37].

Free radicals and oxidative stress have been implicated in the pathogenesis of osteoporosis [38] which is clearly indicated here through in the marked decline in the serum catalase level. Manolagas [34] reported that the administration of catalase prevented ovariectomy-induced bone loss in rats. Therefore, it has been speculated that compounds with antioxidant properties represent promising candidates for the prevention and treatment of osteoporosis. Presently, the carotenoid fraction of *H. pluvialis* restored the serum level of catalase to its normal value. This effect is attributed to the potent anti-oxidant property of astaxanthin-rich carotenoid fraction which has been previously investigated in our Lab. This is due to its modulatory role of the Nrf2/Keap pathway [8]. Recently, it was documented that AST has an inhibitory effect on osteoclast differentiation in osteoporosis model in ovarectomized mice [6].

Previous analysis of the carotenoid fraction of *H. pluvialis* revealed the presence of astaxanthin, β-carotene, zeaxanthin, lutein and canthaxanthin. Astaxanthin was found to be the major carotenoid. Quantitative analysis revealed the presence of 49.99 mg total astaxanthin per 100 g of the carotenoid fraction of *H. pluvialis* (28.7 mg/100 g free astaxanthin and 21.2 mg/100 g esterified astaxanthin) as well as 15.5 mg/100 g β-carotene ([39,7]). The docking study performed in the presence study has shown a high affinity of astaxanthin towards the OPG-RANKL complex protein.

In the present study, it has been found that treatment of osteoporotic rats with BHP, PHP or CHP depicted a reduction of serum OPG levels as compared to the osteoporotic control group and succeeded to normalize the serum RANKL level. A higher production of RANKL has been previously detected *in-vitro* in cultures of peripheral blood mononuclear cells (PBMC) obtained from osteoporotic women [40].

Bone loss in osteoporotic rats in the current study is attributed to the depression in the RANKL with up regulation in the OPG levels which in turn, leads to depression in osteoclast cell differentiation and bone resorption [29] indicating that astaxanthin-rich *H. pluvialis* has a

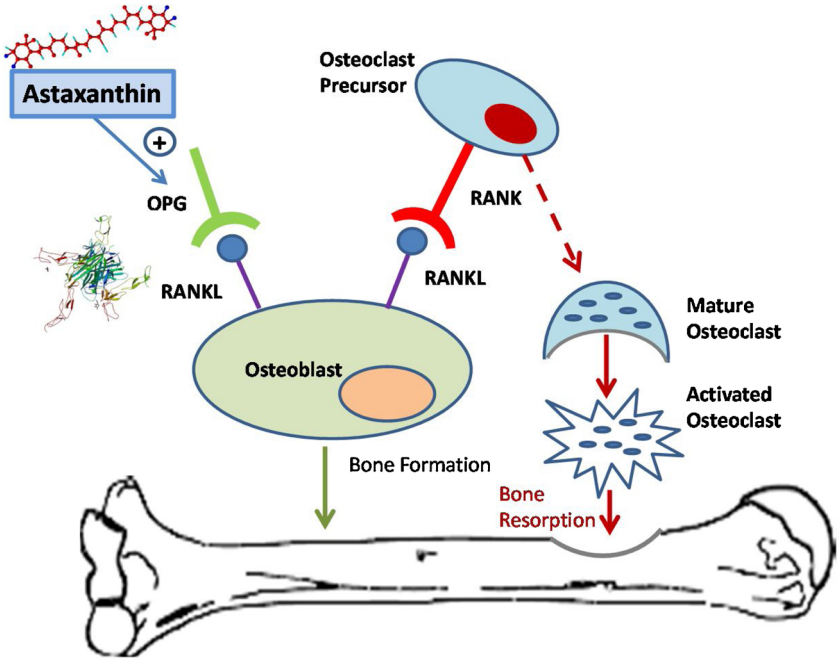


**Fig. 10.** Hypothesis of mechanism of action of astaxanthin-rich *H. pluvialis* on RANK/RANKL/OPG pathway in bone remodeling in D-galactose-induced osteoporotic rats.

regulatory effect on OPG/RANKL pathway which is confirmed by astaxanthin's high affinity towards the OPG-RANKL complex protein that has been revealed by the docking study. The proposed mechanism of action of astaxanthin-rich *H. pluvialis* on RANK/RANKL/OPG pathway in bone remodeling has been illustrated in Fig. 10.

In conclusion, astaxanthin-rich *H. pluvialis* fraction showed to be beneficial in the control of age-related osteoporosis not only through preserving bone mass and serum calcium/phosphorus level but also through increase in the bone mineralization rate. This effect is most likely to be exerted via the regulation of OPG/RANKL expression; promotion of RANKL and inhibition of OPG.

## The conflict of interests

The authors declare no conflict of interest.

## References

[1] J. Woo, T. Kwok, J. Leung, N. Tang, Dietary intake, blood pressure and osteoporosis, J. Hum. Hypertens. 23 (7) (2009) 451–455.
[2] S. Khosla, B.L. Riggs, Pathophysiology of age-related bone loss and osteoporosis, Endocrinol. Metab. Clin. North Am. 34 (4) (2005) 1015–1030 xi.
[3] S.C. Manolagas, A.M. Parfitt, What old means to bone, Trends Endocrinol. Metab. 21 (6) (2010) 369–374.
[4] J. Long, X. Wang, H. Gao, Z. Liu, C. Liu, M. Miao, et al., D-galactose toxicity in mice is associated with mitochondrial dysfunction: protecting effects of mitochondrial nutrient R-alpha-lipoic acid, Biogerontology 8 (3) (2007) 373–381.
[5] E. Grimaud, L. Soubigou, S. Couillaud, P. Coipeau, A. Moreau, N. Passuti, et al., Receptor activator of nuclear factor kappaB ligand (RANKL)/osteoprotegerin (OPG) ratio is increased in severe osteolysis, Am. J. Pathol. 163 (5) (2003) 2021–2031.
[6] Y.H. Hwang, K.J. Kim, S.J. Kim, S.K. Mun, S.G. Hong, Y.J. Son, S.T. Yee, Suppression Effect of Astaxanthin on Osteoclast Formation *In Vitro*and Bone Loss In Vivo, Int. J. Mol. Sci. 19 (2018).
[7] F.K. El-Baz, R.A. Hussein, K. Mahmoud, S.M. Abdo, Cytotoxic activity of carotenoid rich fractions from *Haematococcus pluvialis* and *Dunaliella salina* microalgae and the identification of the phytoconstituents using LC-DAD/ESI-MS, Phytotherapy Res.: PTR 32 (2018) 298–304.
[8] F.K. El-Baz, R.A. Hussein, G.A.R. Abdel Jaleel, D.O. Saleh, Astaxanthin-rich *Haematococcus pluvialis* algal hepatic modulation in D-Galactose-Induced aging in rats: role of Nrf2, Adv. Pharm. Bull. 8 (2018) 523–528.
[9] Y.T. Hung, M.A. Tikhonova, S.J. Ding, P.F. Kao, H.H. Lan, J.M. Liao, et al., Effects of chronic treatment with diosgenin on bone loss in a D-galactose-induced aging rat model, Chin. J. Physiol. 57 (3) (2014) 121–127.
[10] S.A. Goonasekera, J. Davis, J.Q. Kwong, F. Accornero, L. Wei-LaPierre, M.A. Sargent, et al., Enhanced Ca(2)(+) influx from STIM1-Orai1 induces muscle pathology in mouse models of muscular dystrophy, Hum. Mol. Genet. 23 (14) (2014) 3706–3715.
[11] H. Dai, Y.P. Pang, M. Ramirez-Alvarado, S.H. Kaufmann, Evaluation of the BH3-only protein Puma as a direct Bak activator, J. Biol. Chem. 289 (1) (2014) 89–99.
[12] R. Tahtela, J. Seppanen, K. Laitinen, A. Katajamaki, J. Risteli, M.J. Valimaki, Serum tartrate-resistant acid phosphatase 5b in monitoring bisphosphonate treatment with clodronate: a comparison with urinary N-terminal telopeptide of type I collagen and serum type I procollagen amino-terminal propeptide, Osteoporos. int. 16 (9) (2005) 1109–1116.
[13] B. Pineda, P. Laporta, A. Cano, M.A. Garcia-Perez, The Asn19Lys substitution in the osteoclast inhibitory lectin (OCIL) gene is associated with a reduction of bone mineral density in postmenopausal women, Calcif. Tissue Int. 82 (5) (2008) 348–353.
[14] L.C. Hofbauer, M. Schoppet, P. Schuller, V. Viereck, M. Christ, Effects of oral contraceptives on circulating osteoprotegerin and soluble RANK ligand serum levels in healthy young women, Clin. Endocrinol. (Oxf) 60 (2004) 214–219.
[15] H. Aebi, Catalase in vitro, Meth. Enzymol. 105 (1984) 121–126.
[16] C.R. Wheeler, J.A. Salzman, N.M. Elsayed, S.T. Omaye, D.W. Korte Jr., Automated assays for superoxide dismutase, catalase, glutathione peroxidase, and glutathione reductase activity, Anal. Biochem. 184 (2) (1990) 193–199.
[17] L.G. Raisz, G.A. Rodan, Pathogenesis of osteoporosis, Endocrinol. Metab. Clin. North Am. 32 (1) (2003) 15–24.
[18] O. Demontiero, C. Vidal, G. Duque, Aging and bone loss: new insights for the clinician, Ther. Adv. Musculoskelet. Dis. 4 (2) (2012) 61–76.
[19] T. Miyazaki, T. Matsunaga, S. Miyazaki, S. Hokari, T. Komoda, Changes in receptor activator of nuclear factor-kappaB, and its ligand, osteoprotegerin, bone-type alkaline phosphatase, and tartrate-resistant acid phosphatase in ovariectomized rats, J. Cell. Biochem. 93 (3) (2004) 503–512.
[20] X. Sun, J. Liang, C. Wang, S. Cao, Y. Hu, X. Xu, Transient effect of 17beta-estradiol on osteoporosis in ovariectomized rats accompanied with unilateral disuse in the early phase, Int. J. Med. Sci. 12 (5) (2015) 423–431.
[21] Z. Zhang, Y. Chen, L. Xiang, Z. Wang, G.G. Xiao, D. Ju, Diosgenin protects against alveolar bone loss in ovariectomized rats via regulating long non-coding RNAs, Exp. Ther. Med. 16 (5) (2018) 3939–3950.
[22] J.C. Gallagher, B.L. Riggs, J. Eisman, A. Hamstra, S.B. Arnaud, H.F. DeLuca, Intestinal calcium absorption and serum vitamin D metabolites in normal subjects and osteoporotic patients: effect of age and dietary calcium, J. Clin. Invest. 64 (3) (1979) 729–736.
[23] J.C. Gallagher, The pathogenesis of osteoporosis, Bone Miner. 9 (3) (1990) 215–227.
[24] N. Danilovich, P.S. Babu, W. Xing, M. Gerdes, H. Krishnamurthy, M.R. Sairam, Estrogen deficiency, obesity, and skeletal abnormalities in follicle-stimulating hormone receptor knockout (FORKO) female mice, Endocrinology 141 (11) (2000) 4295–4308.
[25] A.M. Shaman, S.R. Kowalski, Hyperphosphatemia management in patients with chronic kidney disease, Saudi Pharm. J. 24 (4) (2016) 494–505.
[26] A.J. Lee, S. Hodges, R. Eastell, Measurement of osteocalcin, Ann. Clin. Biochem. 37 (Pt 4) (2000) 432–446.
[27] M.J. Seibel, Biochemical markers of bone turnover: part I: biochemistry and variability, Clinical biochem. Rev. 26 (2005) 97–122.
[28] K.K. Ivaska, T.A. Hentunen, J. Vaaraniemi, H. Ylipahkala, K. Pettersson,

H.K. Vaananen, Release of intact and fragmented osteocalcin molecules from bone matrix during bone resorption *in vitro*, J. Biolo. Chemestry 279 (18) (2004) 18361–18369.
[29] N. Li, Y. Tu, Y. Shen, Y. Qin, C. Lei, X. Liu, Calycosin attenuates osteoporosis and regulates the expression of OPG/RANKL in ovariectomized rats via MAPK signaling, Pharmazie 71 (10) (2016) 607–612.
[30] Z.M. Chu, H.B. Li, S.X. Sun, Y.C. Jiang, B. Wang, Y.F. Dong, Melatonin promotes osteoblast differentiation of bone marrow mesenchymal stem cells in aged rats, Eur. Rev. Med. Pharmacol. Sci. 21 (19) (2017) 4446–4456.
[31] M. Liu, H. Xu, Y. Ma, J. Cheng, Z. Hua, G. Huang, Osteoblasts proliferation and differentiation stimulating activities of the main components of epimedii folium, Pharmacogn. Mag. 13 (49) (2017) 90–94.
[32] H. Agustina, I. Asyifa, A. Aziz, B.S. Hernowo, The role of osteocalcin and alkaline phosphatase immunohistochemistry in osteosarcoma diagnosis, Patholog. Res. Int. 2018 (2018) 6346409, https://doi.org/10.1155/2018/6346409.
[33] X. Zhu, J. Luo, X. Chen, J. Wang, G. Wang, H. Li, et al., Expression characteristic and significance of interleukin-6, nuclear factor kappa beta, and bone formation markers in rat models of osteoporosis, Trans. Res. 152 (1) (2008) 18–23.
[34] S.C. Manolagas, From estrogen-centric to aging and oxidative stress: a revised perspective of the pathogenesis of osteoporosis, Endocr. Rev. 31 (3) (2010) 266–300.
[35] C.J. Edwards, E. Williams, The role of interleukin-6 in rheumatoid arthritis-associated osteoporosis, Osteoporos. Int. 21 (8) (2010) 1287–1293.
[36] B. Remeniuk, T. King, D. Sukhtankar, A. Nippert, N. Li, F. Li, et al., Disease modifying actions of interleukin-6 blockade in a rat model of bone cancer pain, Pain 159 (4) (2018) 684–698.
[37] S.J. Lee, S.K. Bai, K.S. Lee, S. Namkoong, H.J. Na, K.S. Ha, et al., Astaxanthin inhibits nitric oxide production and inflammatory gene expression by suppressing I (kappa)B kinase-dependent NF-kappaB activation, Mol. Cells 16 (1) (2003) 97–105.
[38] D.W. Zhang, H. Deng, W. Qi, G.Y. Zhao, X.R. Cao, Osteoprotective effect of cordycepin on estrogen deficiency-induced osteoporosis *in vitro* and *in vivo*, Biomed Res. Int. (2015) 423869.
[39] F.K. El-Baz, H.F. Aly, D.B. Fayed, *Dunaliella salina* improved obesity-associated inflammation and oxidative damage in animals' rodent, Asian J. Pharma. Clinical Res. 11 (2018) 240–264.
[40] P. D'Amelio, A. Grimaldi, G.P. Pescarmona, C. Tamone, I. Roato, G. Isaia, Spontaneous osteoclast formation from peripheral blood mononuclear cells in postmenopausal osteoporosis, FASEB J. 19 (3) (2005) 410–412.